THE JOURNAL OF BIOLOGICAL CHEMISTRY VOL. 287, NO. 50, pp. 41979–41990, December 7, 2012

The Assembly of Nonadhesive Fibrinogen Matrices Depends on the αC Regions of the Fibrinogen Molecule*[S]

Received for publication, August 16, 2012, and in revised form, October 16, 2012 Published, JBC Papers in Press, October 18, 2012, DOI 10.1074/jbc.M112.410696

Ivan S. Yermolenko[‡§], Oleg V. Gorkun[¶], Alexander Fuhrmann[‖], Nataly P. Podolnikova[‡], Valeryi K. Lishko[‡], Stanislav P. Oshkadyerov[§], Susan T. Lord[¶], Robert Ros[**], and Tatiana P. Ugarova[‡1]

From the [‡]School of Life Sciences and [**]Department of Physics, Arizona State University, Tempe, Arizona 85287, the [¶]Department of Pathology and Laboratory Medicine, University of North Carolina, Chapel Hill, North Carolina 37599, the [‖]Department of Bioengineering, University of California San Diego, La Jolla, California 92093, and the [§]Institute for Metal Physics, National Academy of Sciences of Ukraine, Kiev 03680, Ukraine

Background: Surface-induced aggregation of fibrinogen results in the assembly of an extensible multilayered matrix, which prevents integrin-mediated cell adhesion.
Results: Without the αC regions, the fibrinogen molecules assemble a defective, poorly extensible matrix supporting sustained cell adhesion.
Conclusion: The assembly of nonadhesive fibrinogen multilayer requires the αC regions of the molecule.
Significance: The molecular mechanism for the assembly of the fibrinogen multilayer is identified.

Adsorption of fibrinogen on fibrin clots and other surfaces strongly reduces integrin-mediated adhesion of platelets and leukocytes with implications for the surface-mediated control of thrombus growth and blood compatibility of biomaterials. The underlying mechanism of this process is surface-induced aggregation of fibrinogen, resulting in the assembly of a nanoscale multilayered matrix. The matrix is extensible, which makes it incapable of transducing strong mechanical forces via cellular integrins, resulting in insufficient intracellular signaling and weak cell adhesion. To determine the mechanism of the multilayer formation, the physical and adhesive properties of fibrinogen matrices prepared from human plasma fibrinogen (hFg), recombinant normal (rFg), and fibrinogen with the truncated αC regions (FgAα251) were compared. Using atomic force microscopy and force spectroscopy, we show that whereas hFg and rFg generated the matrices with a thickness of ~8 nm consisting of 7–8 molecular layers, the deposition of FgAα251 was terminated at two layers, indicating that the αC regions are essential for the multilayer formation. The extensibility of the matrix prepared from FgAα251 was 2-fold lower than that formed from hFg and rFg. In agreement with previous findings that cell adhesion inversely correlates with the extensibility of the fibrinogen matrix, the less extensible FgAα251 matrix and matrices generated from human fibrinogen variants lacking the αC regions supported sustained adhesion of leukocytes and platelets. The persistent adhesiveness of matrices formed from fibrinogen derivatives without the αC regions may have implications for conditions in which elevated levels of these molecules are found, including vascular pathologies, diabetes, thrombolytic therapy, and dysfibrinogenemia.

The plasma protein fibrinogen plays a central role in normal hemostasis and wound healing. During blood vessel injury, fibrinogen is converted into fibrin, which forms a mechanical scaffold of blood clots that seal the breach and prevent blood loss. The conversion of fibrinogen into fibrin is mainly initiated by aggregated platelets, which assemble the prothrombinase complex on their surface, resulting in thrombin generation. Recent advances in optical instrumentation have revealed that fibrin is concentrated within a "fibrin cap" on the surface of thrombi (1, 2). Because fibrin supports strong integrin-mediated adhesion of both platelets and leukocytes *in vitro* (3–6), it should be expected to promote accumulation of these cells on the surface of blood clots *in vivo*. However, numerous studies using traditional staining methods, isotopes, and electron microscopy (7–9) as well as recent studies using new imaging techniques (1, 2) have not detected platelets on the surface of fibrin. Moreover, previous reports have documented that the surface of implanted vascular grafts, which is exposed to flowing blood and invariably coated with fibrin, remains acellular over the years after implantation (10). The anti-adhesive mechanisms that protect the fibrin cap of hemostatic clots and the lumenal fibrin of implanted biomaterials from the excessive accumulation of blood cells *in vivo* are poorly understood.

The surface of fibrin clots in circulation is continuously exposed to high concentrations of fibrinogen. It is well established that fibrinogen forms complexes with fibrin (11) and can self-associate without thrombin activation, forming aggregates (12). We have recently identified a new nanoscale fibrinogen-dependent process, which may contribute to the natural anti-adhesive mechanisms operating on the surface of fibrin clots. In particular, pretreatment of fibrin clots with fibrinogen or its adsorption on various hard surfaces dramatically reduces adhesion of leukocytes and platelets under both static and flow conditions (6, 13). The reduced cell adhesion to fibrin in the presence of physiological concentrations of fibrinogen has also been reported by others (5, 14). The mechanism by which fibrinogen renders hard surfaces nonadhesive is based on the formation of

* This work was supported, in whole or in part, by National Institutes of Health Grant HL107539 (to T. P. U. and R. R.). This work was also supported by a Predoctoral Fellowship from the American Heart Association (to Y. I. S.).
[S] This article contains supplemental Figs. 1S and 2S.
[1] To whom correspondence should be addressed. E-mail: Tatiana.Ugarova@asu.edu.

a "soft" multilayered matrix characterized by weak adhesion forces (13, 15). The origin of the nonadhesive properties of the multilayer lies in its extensibility and inability to transduce strong mechanical forces via integrin receptors, which results in insufficient intracellular signaling and weak cell spreading (13). By contrast, the fibrinogen molecules that are directly attached to hard surfaces forming a non-extensible monolayer support strong cell adhesion. The transition from the monolayer to a bilayer leads to increased matrix extensibility and is accompanied by a sharp decrease in cell adhesion (15). Although the relationship between the multilayer assembly and reduced force generation is clearly established, the molecular basis for the formation of the nonadhesive fibrinogen matrix is unknown.

Fibrinogen is a 340-kDa glycoprotein with a symmetrical dimeric structure consisting of two sets of three polypeptide chains: Aα, Bβ, and γ (Fig. 1*A*). The polypeptide chains are arranged into three regions, with two peripheral D regions being connected to a central E region through the coiled-coil connectors. Each D region consists of the COOH-terminal portions of the Bβ and γ chains, which form the independently folded γC and βC domains as well as a portion of the Aα chain. The last two-thirds of each Aα chain (residues 221–610 in human fibrinogen) form the flexible αC regions, which fold back and are noncovalently tethered to the E region. The αC regions can dissociate from the E region after activation of fibrinogen by thrombin, which cleaves short fibrinopeptides A and B from the N termini of the Aα and Bβ chains, respectively (16–19). The release of the fibrinopeptides results in the exposure of new polymerization sites that interact with the complementary sites constitutively available in the γC and βC domains of the D region, leading to the formation of highly ordered fibrin polymers (20). In addition to these primary strong interactions, other weak interactions may play a role in the assembly of fibrin, including the αC-αC (17), γC-γC, and γC-βC interactions (21) between the neighboring molecules in the fiber. These binding sites do not require thrombin activation and may potentially be involved in self-association of intact fibrinogen in the absence of thrombin activation, a process that occurs under certain experimental conditions (12).

To gain an understanding of the molecular basis for the assembly of the nonadhesive fibrinogen matrix, we have tested the hypothesis that the αC regions contribute to the formation of the multilayer. Using a previously developed methodology based on atomic force microscopy (AFM)[2] (13, 15), we have examined the formation of matrices from intact fibrinogen and its derivatives with the αC regions truncated. We found that the αC regions are indispensable for the assembly of the fibrinogen multilayer. Without the αC regions, the molecules assembled an incomplete, poorly extensible matrix, which supported sustained cell adhesion. Because elevated levels of fibrinogen derivatives lacking the αC portions occur in a number of pathologies and because natural fibrinogen mutants with the αC regions truncated have been associated with thrombosis and/or bleeding, the data suggest that the persistent adhesiveness of the αC-deficient matrices may contribute to complications of thrombosis and thrombolysis.

[2] The abbreviations used are: AFM, atomic force microscopy; hFg, human plasma fibrinogen; rFg, recombinant normal fibrinogen; FgAα251, fibrinogen with truncated αC regions; HMW-Fg, high molecular weight fibrinogen with both αC regions present; LMW-Fg, low molecular weight fibrinogen with one αC region degraded; LMW′-Fg, low molecular weight fibrinogen with both αC regions degraded.

EXPERIMENTAL PROCEDURES

Proteins—Human fibrinogen (hFg) depleted of fibronectin and plasminogen was obtained from Enzyme Research Laboratories (South Bend, IN). In addition, fibrinogen was purified from a pooled outdated human plasma using precipitation with β-alanine (22). Fibrinogen was treated with iodoacetamide to inactivate the residual Factor XIII and then dialyzed against phosphate-buffered saline (PBS). Fibrinogen was labeled with ^{125}I using IODO-GEN (Thermo Scientific Pierce), dialyzed against PBS, and stored at −20 °C. Recombinant normal (rFg; 340 kDa) and fibrinogen with the truncated αC regions (FgAα251; 260 kDa) in which the Aα chain is terminated at Thr-251, were produced as previously described (23). The protein concentration was determined by spectrophotometry at 280 nm using the extinction coefficient 1.51 at 1 mg/ml for hFg and 1.6 for rFg and FgAα251. The two fibrinogen fractions, HMW-Fg (intact high molecular weight fibrinogen with both αC regions present; 340 kDa) and LMW′-Fg (low molecular weight fibrinogen with both αC regions removed; 270 kDa) were purified using ammonium sulfate as described (22). Fibrinogen isolated from outdated plasma using β-alanine precipitation was a source of the fibrinogen fractions because it contained a higher proportion of LMW′-Fg than the commercially available protein.

Preparation of Fibrinogen Matrices—To determine the number of fibrinogen molecules deposited in the multilayer, different concentrations of ^{125}I-labeled hFg (1–100 μg/ml) in PBS were incubated with freshly cleaved mica squares (8 × 8 mm^2). As previously determined, at 0.05–3 μg/ml of added fibrinogen, the surface of mica is saturated with the protein after 3 h at 37 °C (15). Therefore, 3 h was selected as the incubation time for the adsorption of fibrinogen at higher concentrations. Excess fibrinogen was removed by rinsing the mica with water, the bound fibrinogen was determined in a γ-counter, and the number of molecules per μm^2 of surface area was calculated. The samples for AFM were prepared by adsorption of different concentrations of fibrinogen (0.6–100 μg/ml) in PBS onto freshly cleaved mica under the same conditions. The samples were rinsed with water and dried with argon gas.

AFM Imaging of Fibrinogen and Nanolithography—Images in air were acquired using an Agilent 5500 scanning probe microscope (Agilent Technologies, Chandler, AZ) as described previously (24). Imaging was conducted in the amplitude modulation oscillatory mode using Si probes PPP-NCH (Nanosensors) with stiffness in the 10–130 newtons/m range (average 42 newtons/m). The operation at low levels of tip-sample force interactions was further optimized by using smaller operating amplitudes (1–3 nm). The scanners were calibrated as described (24). The experiments were conducted under ambient conditions using a scan rate of 0.6–1.2 Hz. Image analyses (cross-sections) were performed using Gwyddion version 2.10 software as described (15).

The thickness of fibrinogen matrices deposited on mica was determined using the nanolithography procedure described previously (13). Briefly, the areas (3×3 or 5×5 μm^2) were scanned in the contact mode using PPP-NCH AFM probes, pushing away the adsorbed material to generate a "window." To ensure that mica was not damaged, consecutive scans of 5×5-, 5×4-, 5×3-, 5×2-, and 5×1-μm^2 areas as well as two additional 1.2×6-μm^2 and 0.6×6-μm^2 perpendicular scans in the AM mode were made. The height difference between the fibrinogen layer and the cleaned area corresponding to the thickness of the fibrinogen layer was measured.

Molecular Force Spectroscopy—Force-distance measurements of fibrinogen substrates were performed in PBS at 28 °C using an MFP-3D atomic force microscope (Asylum Research, Santa Barbara, CA) essentially as described (13, 15). Silicon nitride probes (MLCT, Veeco Probes, Camarillo, CA) with nominal spring constants in the range of 0.015–0.020 newton/m were used. The probes were calibrated using the built-in function of the instrument. The surfaces coated with different concentrations of fibrinogen were probed using a force trigger of 600 piconewtons and an approach and retract velocity of 2 μm/s. Two 64×64 arrays with a total number of 8192 force-distance curves were collected for each surface measurement. Each curve was analyzed by a custom program written in IGOR Pro 6 (Wavemetrics, Lake Oswego, OR), which calculates the maximal interaction distances and adhesion energies. To obtain mean values of these parameters, the data were fitted using log-normal distributions.

Adhesion Assays—U937 monocytic cells were obtained from the American Tissue Culture Collection and cultured in RPMI 1640 supplemented with 10% fetal bovine serum. Platelets were collected from aspirin-free human blood and isolated by gel filtration as described (25). Freshly cleaved mica surfaces (8×8 mm^2) were placed in 6-well dishes, incubated with different concentrations of fibrinogen for 3 h at 37 °C, and post-coated with 1% BSA (for U937 cells) or 1% polyvinylpyrrolidone (for platelets). 3-ml aliquots (3×10^5/ml) of U937 cells in Hanks' balanced salt solution plus 0.1% BSA or platelets in isotonic Hepes buffer plus 0.1% BSA were added to mica. After a 30- or 50-min incubation at 37 °C for U937 and platelets, respectively, the non-adherent cells were removed by dipping the surfaces into PBS. Photographs of five fields for each surface were taken with the ×20 or ×40 objectives of a Leica DM4000 B microscope (Leica Microsystems, Buffalo Grove, IL), and the number of adherent cells was counted. In selected experiments, morphological features of cells adherent to different substrates were examined by staining for the actin cytoskeleton. The cells were fixed with 4% paraformaldehyde in PBS for 10 min, washed twice with PBS, and permeabilized with 0.1% Triton X-100 for 5 min. After washing with PBS, the cells were stained with Alexa Fluor 546 Phalloidin (Invitrogen).

RESULTS

Thickness of Fibrinogen Matrices Prepared from hFg, rFg, and FgAα251—We previously showed that adsorption of hFg on mica induces its assembly and the formation of a nonadhesive multilayered matrix (13, 15). To characterize the process of the multilayer formation further and determine the number of layers, we measured the thickness of the matrix using AFM nanolithography. As shown in Fig. 1*B*, adsorption of hFg at increasing concentrations reached a plateau level at >60 nM (20 μg/ml) after 3 h of incubation and produced a material with a thickness of 7.5 ± 0.6 nm. Further increase in the coating concentrations of fibrinogen (1–4 mg/ml) did not result in the growth of the matrix. Because the height of a single fibrinogen molecule adsorbed on mica as assessed by AFM imaging is 1.1 ± 0.3 nm (24), the matrix may consist of ~7 molecular layers.

To corroborate this finding by an independent method, we determined the number of molecules deposited in the matrix using ^{125}I-labeled hFg. Similar to the nanolithography measurements, adsorption of ^{125}I-hFg reached saturation at >60 nM (Fig. 1*C*). As shown in Fig. 1*C*, 1210 ± 60 molecules were deposited/1 μm^2 at 3 nM (1 μg/ml). This number is consistent with the number of adsorbed molecules determined directly from the AFM images (1100 ± 150). Furthermore, at this concentration, fibrinogen forms a full monolayer in which all molecules are deposited in the horizontal orientation (15). At saturation (300 nM), 9800 ± 1200 molecules were deposited per 1 μm^2; hence, the matrix consists of ~8 layers. Thus, as determined by two approaches, nanolithography and measuring adsorption of ^{125}I-hFg, the fibrinogen multilayer contains ~7–8 layers.

To investigate the possibility that the αC regions of the fibrinogen molecule (Fig. 1*A*) are involved in the formation of the multilayer, increasing concentrations of recombinant FgAα251 were adsorbed on mica, and the thickness of the generated material was determined by nanolithography. As shown in Fig. 1*B*, the thickness of the matrix remained ~2–3 nm in the 19–190 nM (5–50 μg/ml) range of FgAα251 coating concentrations, suggesting that the formation of the multilayer was strongly impaired. As an essential control, normal rFg produced the matrix with a thickness of 7.3 ± 0.7 nm at 150 nM, which is consistent with thickness of the multilayer formed from hFg (Fig. 1*B*). Thus, the results indicate that the αC regions are centrally involved in the construction of the fibrinogen multilayer.

Formation of the Bilayer from FgAα251 Is Impaired—We previously demonstrated that the transition from the fibrinogen monolayer to the bilayer, which occurs in a 3–6 nM (1–2 μg/ml) range of coating concentrations of hFg, initiates a sharp decline in adhesion forces, indicating that the bilayer represents a minimal nonadhesive structure (15). Because the growth of the matrix generated from FgAα251 was halted at 2.3 ± 0.6 nm (Fig. 1*B*), which may correspond to the bilayer, we investigated its structure in detail using the method that was developed to assess the composition of the hFg bilayer (15). The increasing concentrations of FgAα251 were adsorbed on mica, and AFM images were analyzed to determine the surface coverage. The analyses showed that the surface was gradually covered by the fibrinogen molecules in the first layer (in which the molecules are attached directly to mica) and became fully saturated at ~3.5 nM (Fig. 2*A*, *top*). The surface coverage by FgAα251 was similar to that of hFg (Fig. 2*B*, *dashed line*), indicating that the αC regions do not play a critical role in fibrinogen adsorption to mica. Above 3.5 nM, the FgAα251 molecules began to form the second layer. The formation of the second layer was analyzed by

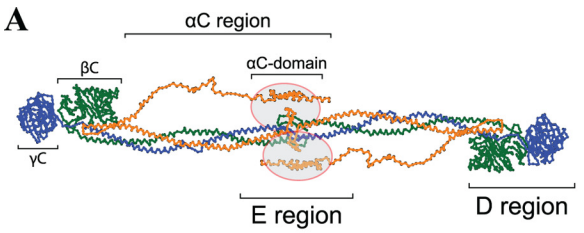

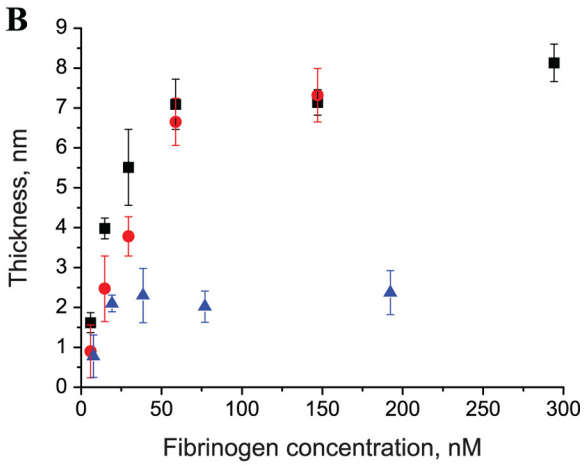

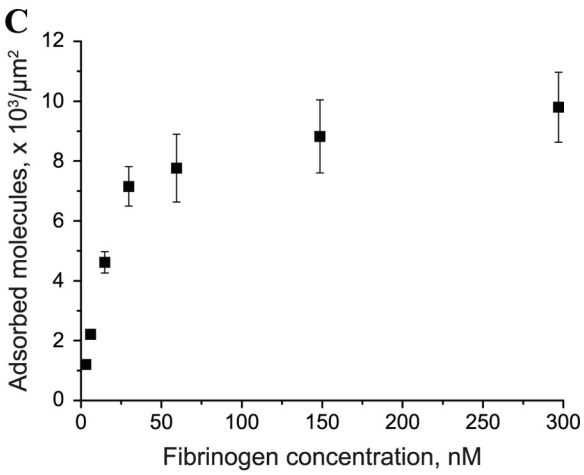

Concentration		
μg/mL	nM	N Molecules
1	3	1210 ± 60
2	6	2210 ± 70
5	15	4600 ± 360
10	29	7200 ± 700
20	59	7800 ± 1100
50	147	8800 ± 1200
100	294	9800 ± 1200

FIGURE 1. **Determination of the thickness of fibrinogen matrices and the number of molecules deposited within them.** *A*, a schematic representation of the domain structure of fibrinogen is based on its crystal structure (49). The three chains (Aα, Bβ, and γ) of the molecule are shown in *orange*, *green*, and *blue*, respectively. The peripheral D regions are composed of the βC and γC domains. FpA and FpB are small fibrinopeptides in the central E region that are cleaved by thrombin. The αC regions consist of a flexible αC connector and the αC domain, which interact with each other and with the E region. *B*, freshly cleaved mica was coated with different concentrations (6–300 nM) of hFg (■), rFg (●), and FgAα251 (▲) for 3 h at 37 °C, and the thickness of the matrices was determined by the nanolithography procedure. The data shown are means ± S.D. (*error bars*) from three experiments with 4–6 surfaces analyzed in each experiment. *C*, different concentrations of ^{125}I-labeled hFg were incubated with mica for 3 h at 37 °C, and the bound fibrinogen was determined in a γ counter. The number of fibrinogen molecules bound per μm^2 of surface area at each coating concentration is shown *below* the graph. The data shown are means ± S.D. of two experiments with triplicate determinations at each experimental point.

applying a mask that approximates the maximum height (~1.1 nm) of the FgAα251 molecules deposited in the monolayer. The mask (shown *below* each image in Fig. 2*A*) hides the molecules in the surface-bound monolayer and allows the visualization of the material in the second layer. The presence of many globular structures in the second layer was observed. As previously proposed (15), these structures most likely represent individual D and E domains of the trinodular fibrinogen molecules protruding from the mica-bound layer (schematically shown in Fig. 2*C*). The calculation of the total area occupied by the FgAα251 molecules showed that the construction of the second layer was impaired compared with that of hFg. For example, whereas the second layer formed by hFg was almost complete at 6 nM, the FgAα251 molecules covered only ~40% of the surface (Fig. 2*B*, *red lines*). The adsorption rate of FgAα251 (12.2 ± 1.9% nM^{-1}) was 2-fold lower than that for hFg (24.4 ± 0.5% nM^{-1}), suggesting that the interaction between the FgAα251 molecules deposited in the surface-bound and upper layers was weakened in the absence of the αC regions.

The Matrices Formed from FgAα251 Are Less Extensible than Those Made from hFg and rFg—We previously reported that adhesion forces that developed between the AFM probe and the fibrinogen bilayer inversely correlate with its extensibility, as assessed from the measurement of adhesion lengths obtained from the force-distance curves (15). We therefore compared the extensibility of the matrices prepared from hFg and FgAα251. Fig. 3 shows several parameters that can be extracted from the force-distance curves that characterize the physical properties of the fibrinogen matrices. The retracting part of a representative force-distance curve obtained on a matrix prepared by adsorption of hFg is shown in Fig. 3*A*. Fig. 3*B* schematically illustrates the events occurring when the AFM tip is in contact with the matrix (*a*) and then retracts from it (*b*–*e*). An adhesive peak at the beginning of the force-distance curve (*c*) reflects the initial detachment of the tip from the surface and is characterized by the adhesion length (*l*). The adhesion length is defined as the point where the cantilever starts bending toward the surface because of the attractive (adhesion) forces and the point where it loses contact with the surface during retraction (but still remains in contact with the matrix). The first adhesive peak is followed by one or more rupture events corresponding to the stretching of the fibrinogen matrix. The force-distance curves usually display several small unbinding events preceding the major rupture events. The abrupt jump in the force curve (d^1–d^2) reflects the last rupture when the tip breaks its association with the substrate and returns to its initial position (d^2 and *e*). The distance at which the AFM tip pulls the fibrinogen matrix from the surface before separating from it is a measure of the substrate extensibility defined as the interaction length.

The analyses of adhesion lengths showed that for the coating concentrations that produce the bilayer matrices (~6–8 nM), normal and αC-truncated fibrinogens exhibited similar values

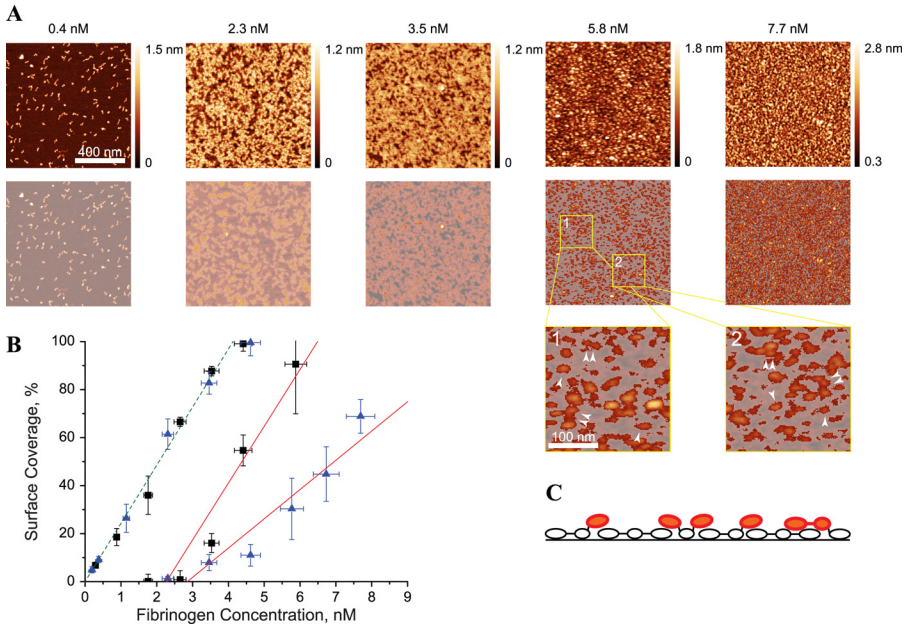

FIGURE 2. **Analyses of the deposition of FgAα251 in the first and second layers.** *A*, AFM images of FgAα251 deposited on mica at various concentrations are shown in the *top row*. *Below* each image is the application of the mask that hides the molecules in the first surface-bound layer, enabling the visualization of the material in the second layer (seen in *red* at 5.8 and 7.7 nM). The height of the immobilized fibrinogen monolayer (1.1 ± 0.3 nm) was selected to generate the mask. Two *enlarged areas* show the material in the second layer for the surface prepared by adsorption of 5.8 nM FgAα251. Note the presence of multiple single (*single arrowheads*) and double (*double arrowheads*) globular domains. *B*, the surface areas covered by FgAα251 (▲) and hFg (■) in the first (*dashed line*) and second (*solid lines*) layers were determined by analyzing the AFM images using Gwyddion 2.10 software as described previously (15). The data are expressed as a percentage of the total surface area. *Vertical bars* represent the S.D. of means of 4–8 images for each fibrinogen concentration from three experiments. *Horizontal error bars* represent the S.D. for each input concentration of fibrinogen estimated as pipette volume variability. *C*, sketch drawn to illustrate the hypothetical orientation of the FgAα251 molecules in the first and second layers based on the images shown in the *boxed areas 1* and *2*. The surface-bound trinodular molecules attached to mica are shown as *open ovals*, and those that are simultaneously attached to mica and protrude in the second layer are shown in *two colors*, with their surface-bound domains shown as *open ovals* and those that protrude shown in *red*.

(2.3 ± 0.9 and 1.9 ± 0.6 nm for hFg and FgAα251, respectively). At higher concentrations (30–150 nM), the matrices produced from hFg were characterized by longer adhesion lengths than those derived from FgAα251 (supplemental Fig. 1S). However, although statistically significant, the differences were small.

In a second set of experiments, we analyzed the maximum interaction lengths. Tracings of force-distance curves collected on matrices prepared by deposition of normal (hFg and rFg) and FgAα251 fibrinogens deposited at 30–40 nM are shown in Fig. 4*A*. Visual inspection of the data revealed that the interaction lengths for the FgAα251 matrix are shorter than those for both normal plasma and recombinant fibrinogens. When plotted as the distribution of interaction lengths, the histograms demonstrated that the FgAα251 matrix is less extensible than those made from both normal fibrinogens: 27.2 ± 3.3, 51.8 ± 7.9, and 49.8 ± 7.8 for FgAα251, hFg, and rFg, respectively (Fig. 4*B*). The most probable interaction lengths of the matrices produced by adsorption of different concentrations of hFg and FgAα251 are shown in Fig. 4*C*. The extensibility of the hFg matrices was 46 ± 6 nm for the bilayer (6 nM) and increased to 57 ± 6 nm for the multilayer (60–150 nM). The extensibility of the rFg matrices was similar to that of hFg. By contrast, the interaction lengths of the matrices generated from FgAα251 remained largely unchanged at all coating concentrations (27.2 ± 3.9 nM), consistent with the finding that the FgAα251 matrix does not grow above two layers. Thus, the matrices formed from normal fibrinogens are ~2 times more extensible that those made from FgAα251.

The area beneath the baseline in the force-distance curves (shown in *green* in Fig. 3*A*) allows for the calculation of the total energy required to detach the AFM tip from the substrate. Twice as much work was needed to separate the tip from the hFg substrate than from the FgAα251 substrate: 1.67 ± 0.5 and 0.88 ± 0.12 aJ for hFg and FgAα251 matrices, respectively. From these estimates, the αC regions may contribute ~50% of the energy required to separate the tip from the hFg bilayer with the remaining energy coming from the interactions between other fibrinogen domains (Fig. 4*D*).

The Matrices Formed from FgAα251 Are Locked in a Permanently Adhesive State—We previously demonstrated an inverse correlation between cell adhesion and growth of the hFg multilayer (13, 15). In particular, the strongest cell adhesion was observed on a monolayer, steeply declined when fibrinogen formed a bilayer, and then continued to decrease as the formation of the multilayer progressed further. Because FgAα251 is not capable of assembling a multilayer, the matrices formed from it may support sustained adhesion. To investigate this possibility, mica was coated with different concentrations of FgAα251 and hFg, and adhesion of U937 monocytic cells was examined. As expected, the adhesion of cells to FgAα251 was the strongest at the coating concentration that produces a monolayer (2.3 nM) and gradually declined in the range 2.3–7.7 nM, coinciding with the formation of the bilayer (Fig. 5*A*). A similar behavior was observed for the adhesion of cells to hFg. However, although cell adhesion continued to decline with the increase in the coating concentration of hFg, it remained largely

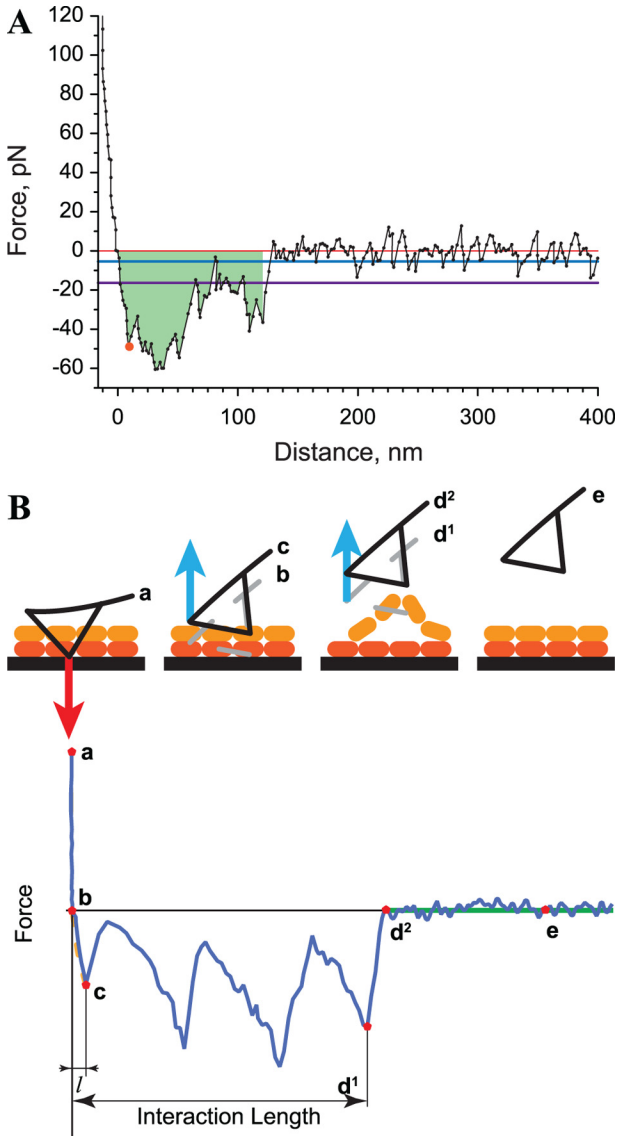

FIGURE 3. **A representation of the experiment for measuring the parameters that characterize the physical properties of the fibrinogen matrices.** *A*, retracting part of representative force-distance curve obtained for the interaction between the AFM tip and the matrix produced by coating mica with hFg (59 nM) using a retracting velocity of 2 μm/s. A *red dot* at the beginning of the force curve marks the adhesion peak. Shown are standard (68.27%; *blue*) and triple standard (99.73%; *purple*) deviation of the cantilever thermal noise fluctuations over base line (*red*) that were calculated to determine the last rupture event and the maximal interaction length. The total energy of the tip-matrix interaction is shown as an area *shaded* in *green* between the base line and the force-distance curve. *B*, a schematic representation of events recorded in the retraction part of the force-distance curve. *a*, the state when the AFM tip indents into the fibrinogen matrix (shown for the bilayer); *b* and *c*, an event when the AFM tip retracts from the surface and the deflection of the tip is recorded; d^1–d^2, the retraction of the tip (shown in *gray*) from the surface with the fibrinogen molecules attached to it, causing stretching of the matrix leading to several intermediate ruptures until the last rupture (d^1) and the detachment of the tip from the matrix (d^2); *e*, the tip returns into its relaxed position. The adhesion peak in the beginning of the force-distance curve (the closest local minimum) reflects adhesion between the tip and the matrix. The adhesion length (*l*) is defined as the point where the tip loses contact with the surface during retraction but is still in contact with the substrate. The distance at which the tip pulls the fibrinogen matrix from the surface before separating from it is defined as the interaction length. The fibrinogen molecules in the surface-bound layer are shown as *red ovals*, and those in the second layer are *colored* in *yellow*. *pN*, piconewtons.

unaffected by the increase in the concentration of FgAα251 (Fig. 5, *A* and *B*). In the 20–60 nM range, where hFg supported only weak cell adhesion (1–3%), adhesion to FgAα251 was 45 ± 5%. When the cell adhesion data were plotted against the thickness of the layer for each fibrinogen concentration, the graph showed that the matrix assembled from four and more layers of hFg was essentially nonadhesive (Fig. 5*C*). At the same time, the matrices formed from FgAα251 supported sustained cell adhesion, reflecting the inability of FgAα251 to assemble the multilayer.

Further evidence for the inability of FgAα251 to produce nonadhesive matrices was obtained in experiments with platelets. Although adhesion of platelets to hFg adsorbed at the increasing concentrations gradually declined, it remained unaffected by the increase in the coating concentrations of FgAα251 (Fig. 6*A* and supplemental Fig. 2S, *A* and *B*). Moreover, microscopic examination of platelets showed that reduced platelet adhesion to hFg coincided with a steady decrease in the extent of platelet spreading (Fig. 6*B* (*top*) and supplemental Fig. 2S*A*). By contrast, platelet spreading on FgAα251 remained virtually the same (Fig. 6*B* (*bottom*) and supplemental Fig. 2S*B*).

The Matrices Formed from Natural Fibrinogen Derivatives Lacking the αC Regions Support Sustained Cell Adhesion—Fibrinogen in circulation is a heterogeneous mixture of molecules characterized by different lengths of the αC region resulting from proteolytic degradation and classified according to their molecular weight as HMW-, LMW-, and LMW′-fibrinogens (26). The proportion of species with the truncated αC regions is elevated in patients with various pathologies (27–29). To verify whether LMW′-Fg containing both αC regions truncated recapitulates the behavior of recombinant FgAα251, fibrinogen isolated from pooled human plasma was fractionated into HMW-Fg and LMW′-Fg (Fig. 7*A*). As assessed by nanolithography, whereas HMW-Fg produced a matrix with a thickness of 7.0 ± 0.7 nm, the maximum thickness of the LMW′-Fg matrix was 3.8 ± 0. 5 nm (Fig. 7*B*). Similar to FgAα251, adsorption of LMW′-Fg at the increased concentrations did not result in the full loss of adhesion of U937 cells (Fig. 7*C*). These results confirm that truncation of the αC regions in plasma fibrinogens hinders the formation of an efficacious nonadhesive substrate.

DISCUSSION

In previous studies, we reported a nanoscale process in which adsorption of fibrinogen on various surfaces produces multilayered matrix with potent antiadhesive properties toward blood cells (13, 15). In this study, we established the molecular basis for its formation. The major finding of this study is that the αC regions of the fibrinogen molecule are essential for the multilayer assembly. In contrast to intact fibrinogen, the fibrinogen molecules without the αC regions fail to assemble a matrix with more than two layers. Moreover, in agreement with previous findings that the assembly of several layers is required to produce a fully nonadhesive matrix, we found that the matrices made from the αC-deficient fibrinogens are locked in a permanently adhesive state.

According to a current view, the αC regions (residues 221–610 of the Aα chains) in human fibrinogen form structures consisting of a relatively compact portion named the αC

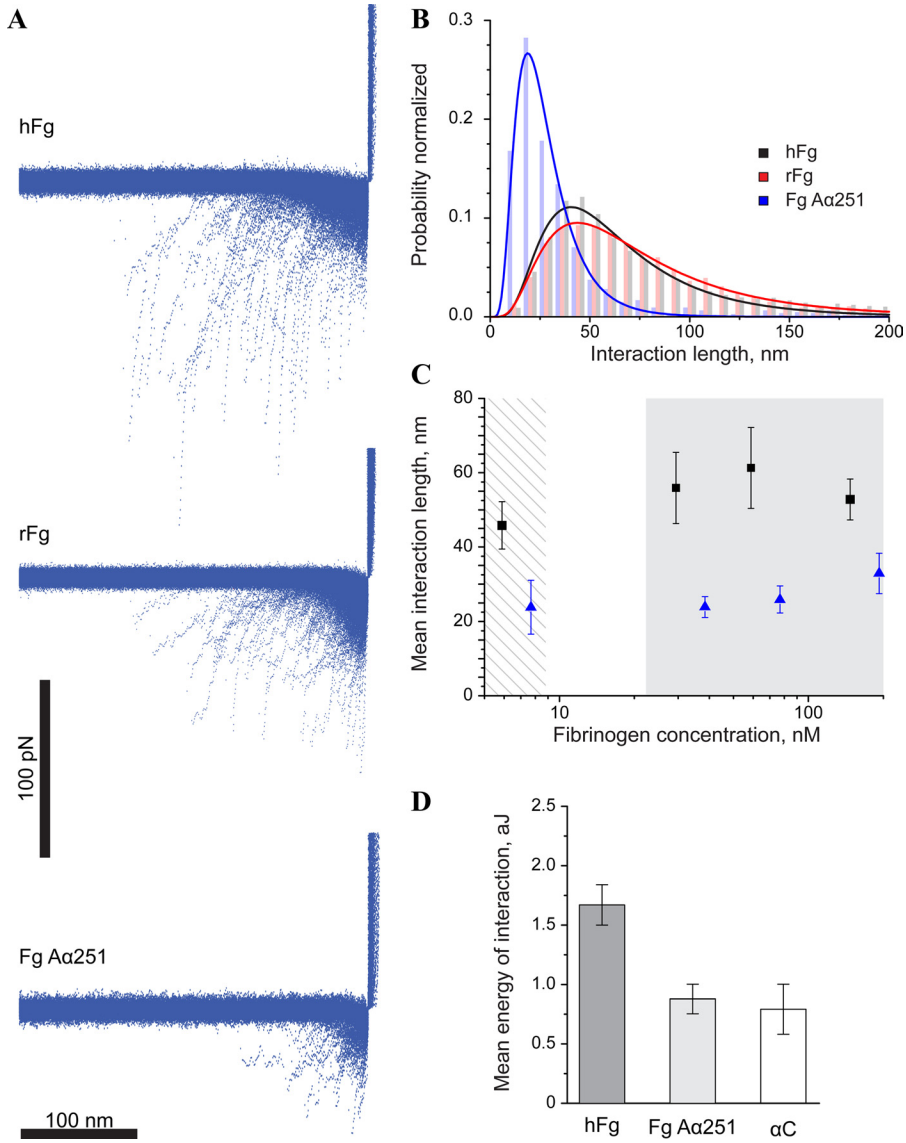

FIGURE 4. **Interaction lengths and energies required to detach the AFM tip from the matrices produced by deposition of hFg, rFg, and FgAα251.** *A*, force-distance curves were derived from a single force map measurement for each matrix produced by deposition of hFg (29 nM), rFg (29 nM), and FgAα251 (38 nM). *B*, representative probability distributions of the interaction lengths for the matrices prepared as described above were generated from the analyses of 4096 force-distance curves (a single array in the force map for each fibrinogen). *C*, the interaction length for the bilayers (*striped area*) and multilayer (*gray area*) prepared from hFg (■) and FgAα251 (▲). Between 15,000 and 32,000 force-distance curves were analyzed for each concentration of fibrinogen. The data shown are means and S.D. (*error bars*) from 2–4 experiments. *D*, the energy of the interaction between the AFM tip and the bilayers prepared from hFg and FgAα251 was calculated from the area *under* the base line in the force-distance curves. The contribution of the αC interactions (*αC*) to the hFg-hFg interactions was calculated by subtracting the value of energy for the FgAα251-AFM tip interactions (protein-protein interactions) from that for the hFg-AFM tip interactions. *aJ*, attojoules.

domain (residues 392–610) attached to the rest of the Aα chain through a flexible unstructured tether, the αC connector (residues 221–391) (30, 31). Numerous biophysical and biochemical data indicate that in the intact molecule, two αC regions interact with each other and with the central E region to create a compact organization (16–18, 32) (Fig. 8*A*). The interaction of the αC regions with the E region is mediated mainly via fibrinopeptides B, although the contribution of fibrinopeptides A has also been shown (19). The binding sites within the αC regions involved in the interactions with fibrinopeptides and self-association have not been established. Nevertheless, the ability of the fragments representing the entire αC region or the αC domain to form oligomers, as well as the reports of αC-αC interactions at the single-molecule level provide direct evidence that they contain the self-association sites (19, 33). The release of fibrinopeptides B by thrombin during the conversion of fibrinogen to fibrin is accompanied by the dissociation of the αC regions from the E region (Fig. 8*A*) and from each other, leading to the formation of the intermolecular links with the neighboring molecules in the growing fibrin polymer (32).

It is also known that adsorption of fibrinogen on various surfaces may induce the dissociation of the αC regions from their central location. This conformational change has directly been shown by electron microscopy studies that visualized the αC regions as extending from the two peripheral D regions of the molecule (16, 32, 34). Moreover, the transition of the αC regions from the "closed" to an "open" state upon fibrinogen adsorption is evidenced by exposure of epitopes for several

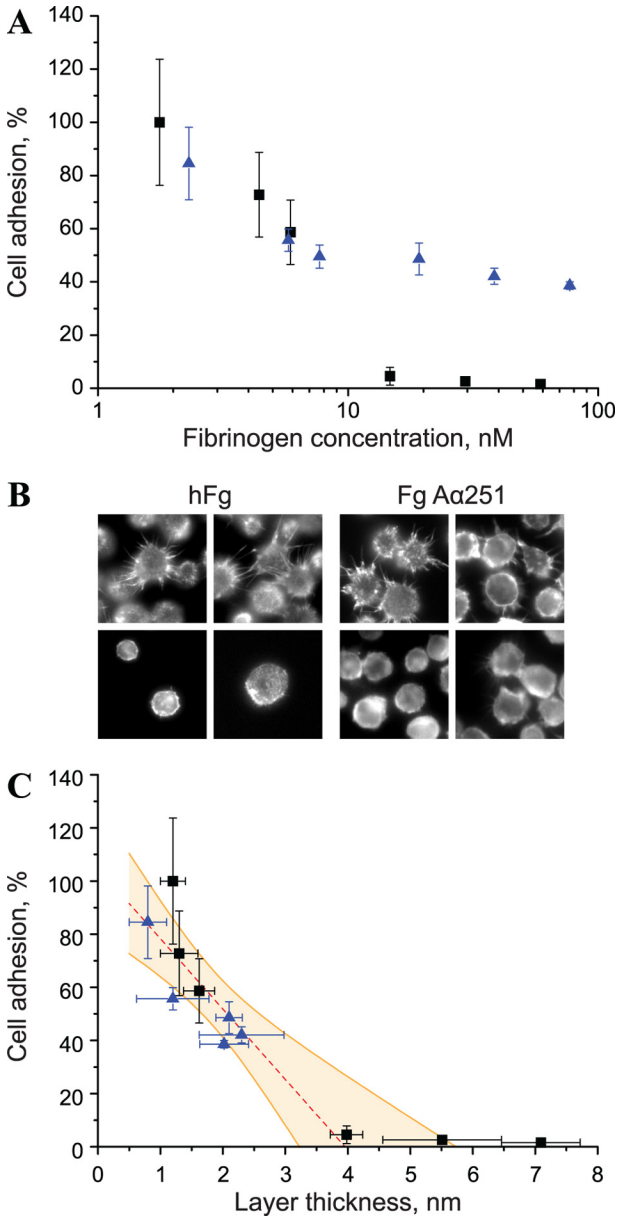

FIGURE 5. **Adhesion of U937 monocytic cells to fibrinogen matrices.** *A*, U937 cells were allowed to adhere to the mica surfaces coated with different concentrations of hFg (■) and FgAα251 (▲). Non-adherent cells were removed by washing, and adherent cells were quantified by taking pictures of five random fields for each surface. Adhesion for both fibrinogens was expressed as a percentage of maximal adhesion to the hFg monolayer (1.8 nM). Data shown are means of triplicate determinations for each concentration of two independent experiments, and *error bars* represent S.D. *B*, cells were stained for actin using Alexa Fluor 546 Phalloidin. *Left panels*, representative images of U937 cells adherent to the surfaces coated with hFg at the concentrations that produce the monolayer (1.8 nM; *two top images*) or multilayer (60 nM; *two bottom images*). *Right panels*, representative images of U937 cells adherent to the surfaces coated with 2.3 nM (monolayer; *two upper images*) and 77 nM (*two bottom images*) of FgAα251. Note that in the 7.7–77 nM range of coating concentrations, FgAα251 does not develop a multilayer. *C*, cell adhesion data in *A* were plotted against the thickness of the fibrinogen matrices. The data for the matrix thickness for each fibrinogen concentration were obtained from Fig. 1. The *shaded area* represents a 95% confidence interval for the linear fit of the experimental data.

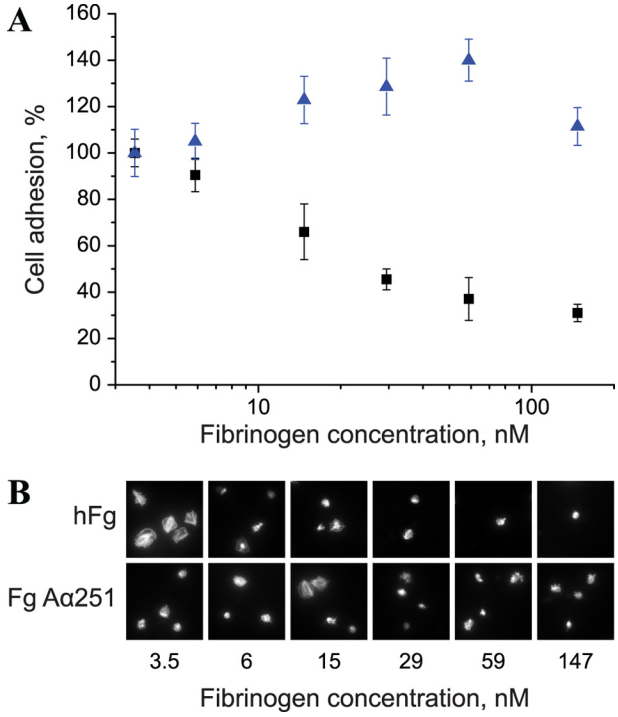

FIGURE 6. **Adhesion of platelets to fibrinogen matrices.** *A*, platelets were allowed to adhere to the surfaces coated with different concentrations of hFg (■) and FgAα251 (▲). Non-adherent cells were removed by washing, and adherent cells were quantified by taking pictures of five random fields for each surface. Photographs were taken with the ×40 objective. Adhesion was expressed as a percentage of platelet adhesion to 3.5 nM for each fibrinogen. Data shown are means of duplicate determinations for each concentration of 3–4 independent experiments, and *error bars* represent S.D. *B*, cells were stained for actin using Alexa Fluor 546 Phalloidin. *Top* and *bottom panels*, representative images of platelets adherent to the increasing concentrations of hFg and FgAα251, respectively. (Please see supplemental Fig. 2S, *A* and *B* for a detailed representation of this figure).

monoclonal antibodies that reside in the coiled-coil connectors of fibrinogen and that are apparently shielded by the interacting αC regions in the intact molecule (25, 35). In addition, immobilization of fibrinogen on the surface results in unmasking of cryptic binding sites for several components of the fibrinolytic system (tissue plasminogen activator and α2-antiplasmin) that reside in the αC regions themselves (36, 37). It is noteworthy that during adsorption on surfaces, the αC regions dissociate from the central E region, although it still contains fibrinopeptides A and B, illustrating the ease with which the αC regions can unfold and the relatively nonspecific nature of the trigger.

The finding of the present study that the formation of the fibrinogen multilayer totally depends on the αC regions suggests a model in which initial contact with the surface induces a conformational change in the surface-bound molecules resulting in the dissociation of the αC regions from the bulk of the molecule and enabling their association with the αC regions of incoming molecules (Fig. 8*B*). The deposition of fibrinogen in the second and posterior layers appears to also result in unfolding of the αC regions to account for the addition of new layers. Furthermore, not only αC-αC, but the interactions between αC and fibrinopeptides A and B, which remain in fibrinogen, may facilitate the association between layers (Fig. 8*B*). Although this model coherently accounts for how the switch from intra- to intermolecular interactions between the αC regions contributes to the multilayer formation, it remains speculative at present, and further studies with fibrinogen variants containing truncated αC regions may help clarify the precise mechanism.

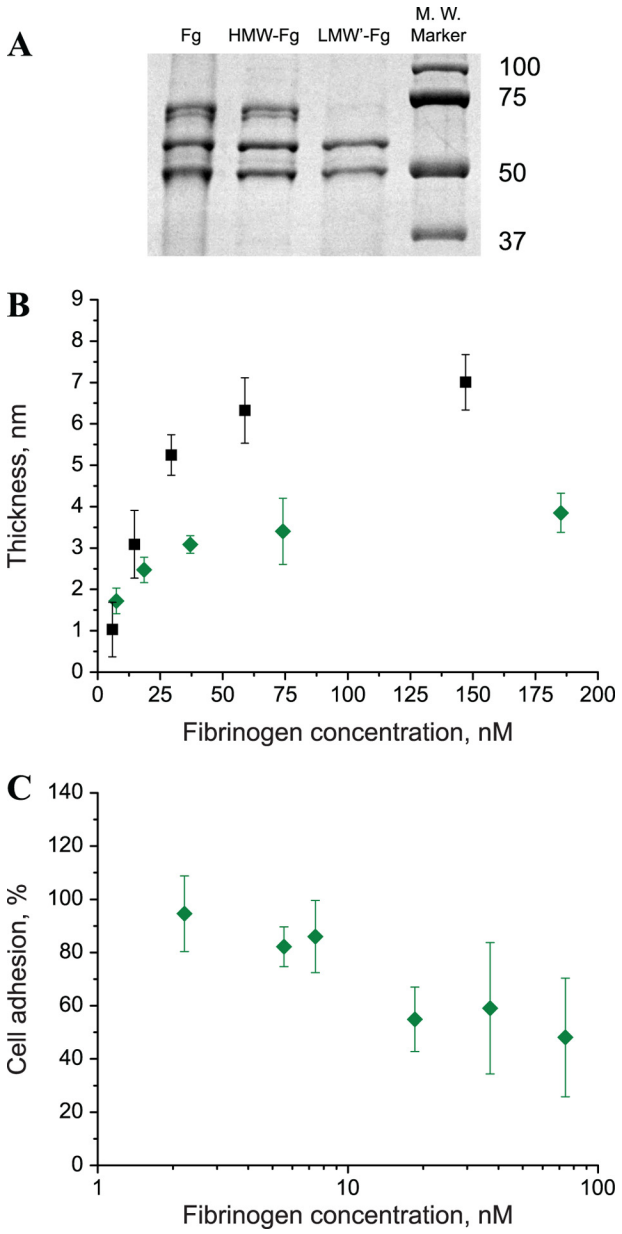

FIGURE 7. **Thickness and adhesive properties of the matrices prepared from the fibrinogen fractions with and without αC regions isolated from human plasma.** *A*, the HMW-Fg (340 kDa) and LMW′-Fg (270 kDa) fractions were isolated from a pooled human plasma and analyzed by SDS-PAGE under reduced conditions (4–15% gradient gel). After reduction, the three intact polypeptide chains Aα, Bβ, and γ in HMW-Fg and only Bβ and γ in LMW′-Fg are seen. The 24-kDa remnant of the Aα chain in LMW′-Fg is not shown in the gel. Molecular weight markers are presented on the *right*. *B*, the thickness of matrices prepared by adsorption of different concentrations of HMW-Fg (■) and LMW′-Fg (♦) was determined by nanolithography. *C*, adhesion of U937 cells to the matrices prepared by adsorption of different concentrations of LMW′-Fg was performed as described in the legend to Fig. 5*A*. Adhesion was expressed as a percentage of maximal adhesion to the monolayer produced from HMW-Fg (1.8 nM). Such presentation of the data allows a direct comparison of cell numbers adherent to HMW- and LMW-Fg monolayers. Data shown are means of triplicate determinations for each concentration of three independent experiments, and *error bars* represent S.D.

The analyses of the force-distance curves demonstrate that the bilayer formed from intact fibrinogen (hFg) is ~1.9-fold more extensible than that generated from the αC-deficient FgAα251 (Fig. 4*C*), indicating that the two layers in hFg can be separated by a longer distance when pulled by the AFM tip. The establishment of bonds between two adjacent layers in the form of longer αC-αC and shorter αC-E links appears to contribute to the increased extensibility of the hFg-hFg bilayer. The even higher extensibility of the multilayer (Fig. 4*C*) evidently reflects its stretching and the separation of the upper layers. Nevertheless, the fact that fibrinogen devoid of the αC regions can form a bilayer structure (Fig. 8*C*) argues for additional protein-protein interactions that may contribute to its construction. The calculations of the energy required to detach the AFM tip from the hFg bilayer suggest that the αC regions contribute ~50% of energy to the interactions between the molecules, with the remaining energy contributed by other interacting parts of the molecules (Fig. 4*D*). The nature of these interactions is unknown. Because adsorption of fibrinogen induces not only unfolding of the αC regions but also elicits unmasking of other sequences (38, 39), it may potentially result in exposure of self-association sites in other parts of the molecule. Alternatively, γC–γC and γC–βC bonds similar to those that have been proposed to exist in the fibrin fibers (21) may occur in the multilayer fibrinogen. However, it is unlikely that these interactions play a dominant role because the surface-induced fibrinogen matrix does not display a regular structure. Nevertheless, despite the potential contribution of protein-protein interactions other than αC regions, the FgAα251 matrix does not grow above two layers, implying that these protein-interactions are not, on their own, able to support the assembly of the full multilayer, leading to the conclusion that the αC regions play a major role in this process.

Our data show that the matrix reaches a maximum height of 7.5 ± 0.6 nm corresponding to 7–8 molecular layers (Fig. 1*B*). These data are in agreement with the AFM measurements by Evans-Nguyen *et al.* (40) of the protein layer prepared by adsorption of 1 mg/ml fibrinogen on hydrophobic surfaces. Although the formation of the multilayer was not considered in that study, the height of the protein film, 5.5 ± 2.2 nm, is close to our data. The finding that the multilayer stops growing suggests that unfolding of the αC regions may occur in a specific manner to account for the construction of such a finite nanoscale structure. One of the possibilities is that the growth of the multilayer is terminated because the number of reactive unfolded αC regions available for self-association decreases gradually with the addition of new layers. Accordingly, the largest number of the αC-mediated links may be formed in the surface-proximal bilayer and then decline in the third layer because only individual αC regions would protrude from the second layer, as schematically shown in Fig. 8*B*. As the multilayer grows, more and more αC regions would be consumed by the interactions within the adjacent layers until no free αC regions are available in the uppermost layer. Another, not mutually exclusive interpretation, is that the degree of unfolding of the αC regions in the upper layers may be limited because the incoming molecules attach to the soft protein matrix rather than to the hard mica surface. This hypothesis, in concert with previous data indicating that the extent of fibrinogen unfolding varies on different surfaces, implies that the process of multilayer formation may be markedly influenced by the selected substratum. Remarkably, some surfaces may even induce an ordered assembly of fibrinogen (41, 42). Recent studies have

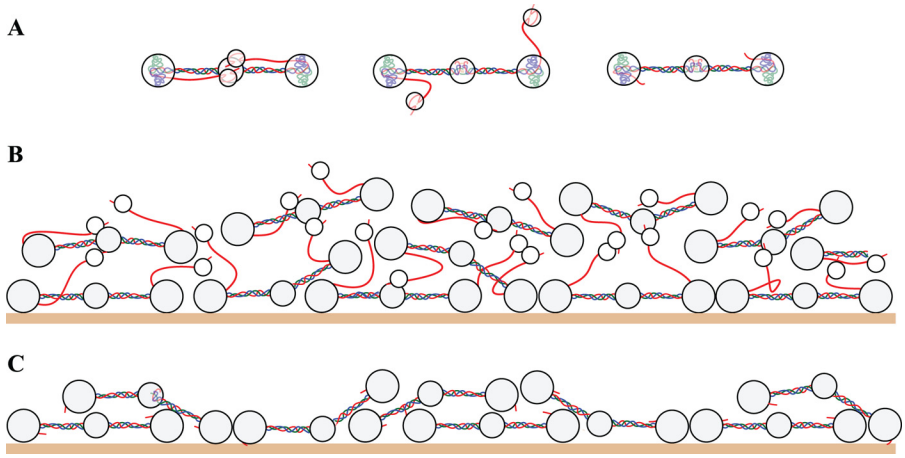

FIGURE 8. **A model of possible interactions between the molecules in the matrix formed by intact hFg and FgAα251.** *A*, a representation of the fibrinogen molecule showing the αC regions in different conformations. The molecule on the *left* is shown in the closed conformation in which the αC regions fold back toward the center of the molecule and interact with each other and the central E domain. The molecule in the *middle* is shown in the open conformation, in which the αC regions dissociate from their central location. The molecule without the αC regions corresponding to FgAα251 and LMW′-Fg is shown on the *right*. *B*, initial steps in the formation of the matrix from intact hFg. The deposition of hFg on the surface induces the conformational change in the αC regions resulting in their dissociation from the E domain and each other, enabling the αC-αC and αC-E interactions between the molecules in the neighboring layers. *C*, FgAα251 with two αC regions lacking is not capable of forming the multilayer.

demonstrated that adsorption of fibrinogen at 4 mg/ml on hydrophobic clay microplates induces the formation of fibers with a height of ~20 nm (42). Interestingly, the assembly of these fibers was dependent on the αC regions. In conjunction with the results presented here, these data indicate that the formation of both the unstructured multilayer and ordered fibrinogen fibers depend on the αC regions.

Another important finding of the present study is that the inability of the matrix generated from FgAα251 to grow creates a permanently adhesive substrate. We have previously showed that the transition from the highly adhesive surface-bound hFg monolayer to the bilayer initiates a sharp decrease in cell adhesion and that further increase in the coating concentration leads to the formation of an essentially nonadhesive matrix (13, 15). The origin of the nonadhesive properties of the multilayer appears to be its enhanced, compared with the monolayer, extensibility, which strongly reduces integrin-mediated mechanotransduction, resulting in weak intracellular signaling and poor cell spreading (15). The correlation between leukocyte adhesion and the number of layers demonstrates that the formation of four hFg layers is sufficient to reduce adhesion by more than 90%, and the subsequent increase in the matrix thickness produces a totally nonadhesive matrix (Fig. 5). Moreover, the assembly of the multilayer effectively reduces platelet adhesion and spreading (Fig. 6 and supplemental Fig. 2S*A*). The finding that the matrix produced from FgAα251 supports sustained adhesion of both leukocytes and platelets is consistent with the inability of the αC-deficient molecules to assemble more than two layers. It should be noted that although cell adhesion generally inversely correlates with the extensibility of the matrix, this relationship was not observed for the hFg and FgAα251 bilayers (*i.e.* despite a 1.9-fold higher extensibility of the hFg bilayer, cell adhesion to both matrices was not statistically different) (Fig. 5, *A* and *C*). The lack of a strong correlation may reflect a relative insensitivity of standard cell adhesion assays compared with the AFM experiments. Furthermore, we consistently observed stronger adhesion of platelets as compared with leukocytes (*i.e.* the hFg multilayer did not eliminate platelet adhesion completely) (Fig. 6*A*). In addition, in contrast to leukocytes, platelets did not sense variations in the composition of the matrix assembled from FgAα251. At present, the differences in adhesion of platelets and leukocytes to the fibrinogen multilayer remain to be defined.

The self-assembly of fibrinogen without thrombin activation is a well known phenomenon that occurs under several experimental conditions (12). Although self-association of fibrinogen is readily induced, suggesting its potential significance, no physiologic role has been ascribed to this process. We have recently proposed that the fibrinogen matrix deposited on the surface of fibrin clots may play an important role in normal hemostasis by preventing excessive adhesion of circulating blood cells, thus limiting thrombus propagation (6, 43). The finding of the present study that the fibrinogen molecules without the αC regions are incapable of developing the multilayer with ensuing sustained cell adhesion may have significant implications with respect to the role of these derivatives in several pathological conditions. It is well known that fibrinogen in circulation is a heterogeneous and variable mixture of molecules characterized by different lengths of the αC regions. Typical plasma-derived fibrinogen contains a major fraction with intact αC regions, HMW-Fg (50–70%), and a minor fraction with one or two αC regions degraded, LMW-Fg and LMW′-Fg, respectively (44, 45). The fraction with both αC regions truncated is elevated in patients with peripheral vascular diseases, liver disease, or diabetes and in the elderly (27–29, 45). A substantial amount of the molecules without the αC regions is produced during thrombolytic therapy (46). Moreover, there are a number of cases of hereditary dysfibrinogenemia in which the αC regions are partially or fully deleted (see the GEHT (Groupe d'Etude sur l'Hémostase et la Thrombose) Web site) (47). Interestingly, in selected dysfibrinogenemias, truncations of the αC regions have been associated with either thrombosis or bleeding, and a few have both bleeding and thrombotic tendencies (47, 48). The mechanisms by which deletions of the αC regions

increase the risk for thrombosis or bleeding are unknown. Traditionally, the bleeding and thrombotic complications caused by the fibrinogen mutants without the αC regions have been explained by their tendency to form clots with an altered architecture. However, it could also be expected that the deposition of these proadhesive molecules on the surface of thrombi may be associated with the increased accumulation of leukocytes, which are known to secrete potent proteolytic enzymes, or platelets, which may lead to thrombus growth. This new aspect of the pathophysiologic function of αC-deficient fibrinogen derivatives remains to be established.

REFERENCES

1. Kamocka, M. M., Mu, J., Liu, X., Chen, N., Zollman, A., Sturonas-Brown, B., Dunn, K., Xu, Z., Chen, D. Z., Alber, M. S., and Rosen, E. D. (2010) Two-photon intravital imaging of thrombus development. *J. Biomed. Opt.* **15,** 016020
2. Cooley, B. C. (2011) *In vivo* fluorescence imaging of large-vessel thrombosis in mice. *Arterioscler. Thromb. Vasc. Biol.* **31,** 1351–1356
3. Wright, S. D., Weitz, J. I., Huang, A. J., Levin, S. M., Silverstein, S. C., and Loike, J. D. (1988) Complement receptor type three (CD11b/CD18) of human polymorphonuclear leukocytes recognizes fibrinogen. *Proc. Natl. Acad. Sci. U.S.A.* **85,** 7734–7738
4. Kuijper, P. H., Gallardo Torres, H. I., van der Linden, J. A., Lammers, J. W., Sixma, J. J., Zwaginga, J. J., and Koenderman, L. (1997) Neutrophil adhesion to fibrinogen and fibrin under flow conditions is diminished by activation and L-selectin shedding. *Blood* **89,** 2131–2138
5. Kuijper, P. H., Torres, G., Lammers, J.-W., Sixma, J. J., Koenderman, L., and Zwaginga, J. J. (1997) Platelet and fibrin deposition at the damaged vessel wall. Cooperative substrates for neutrophil adhesion under flow conditions. *Blood* **89,** 166–175
6. Lishko, V. K., Burke, T., and Ugarova, T. (2007) Anti-adhesive effect of fibrinogen. A safeguard for thrombus stability. *Blood* **109,** 1541–1549
7. Groves, H. M., Kinlough-Rathbone, R. L., Richardson, M., Jørgensen, L., Moore, S., and Mustard, J. F. (1982) Thrombin generation and fibrin formation following injury to rabbit neointima. *Lab. Invest.* **46,** 605–612
8. van Aken, P. J., and Emeis, J. J. (1982) Organization of experimentally induced arterial thrombosis in rats. The first six days. *Artery* **11,** 156–173
9. van Ryn, J., Lorenz, M., Merk, H., Buchanan, M. R., and Eisert, W. G. (2003) Accumulation of radiolabeled platelets and fibrin on the carotid artery of rabbits after angioplasty. Effects of heparin and dipyridamole. *Thromb. Haemost.* **90,** 1179–1186
10. Zilla, P., Bezuidenhout, D., and Human, P. (2007) Prostethic vascular grafts. Wrong models, wrong questions and no healing. *Biomaterials* **28,** 5009–5027
11. Doolittle, R. F. (1984) Fibrinogen and fibrin. *Annu. Rev. Biochem.* **53,** 195–229
12. Gollwitzer, R., Bode, W., and Karges, H. E. (1983) On the aggregation of fibrinogen molecules. *Thromb. Res.*, Suppl. **5,** 41–53
13. Podolnikova, N. P., Yermolenko, I. S., Fuhrmann, A., Lishko, V. K., Magonov, S., Bowen, B., Enderlein, J., Podolnikov, A. V., Ros, R., and Ugarova, T. P. (2010) Control of integrin αIIbβ3 outside-in signaling and platelet adhesion by sensing the physical properties of fibrin(ogen) substrates. *Biochemistry* **49,** 68–77
14. Endenburg, S. C., Lindeboom-Blokzijl, L., Zwaginga, J. J., Sixma, J. J., and de Groot, P. G. (1996) Plasma fibrinogen inhibits platelet adhesion in flowing blood to immobilized fibrinogen. *Arterioscler. Thromb. Vasc. Biol.* **16,** 633–638
15. Yermolenko, I. S., Fuhrmann, A., Magonov, S. N., Lishko V. K., Oshkaderov, S. P., Ros, R., and Ugarova, T. P. (2010) Origin of nonadhesive properties of fibrinogen matrices probed by force spectroscopy. *Langmuir* **26,** 17269–17277
16. Veklich, Y. I., Gorkun, O. V., Medved, L. V., Nieuwenhuizen, W., and Weisel, J. W. (1993) Carboxyl-terminal portions of the α chains of fibrinogen and fibrin. Localization by electron microscopy and the effects of isolated αC fragments on polymerization. *J. Biol. Chem.* **268,** 13577–13585
17. Gorkun, O. V., Veklich, Y. I., Medved, L. V., Henschen, A. H., and Weisel, J. W. (1994) Role of the αC domains of fibrin in clot formation. *Biochemistry* **33,** 6986–6997
18. Gorkun, O. V., Litvinov, R. I., Veklich, Y. I., and Weisel, J. W. (2006) Interactions mediated by the N-terminus of fibrinogen's Bβ chain. *Biochemistry* **45,** 14843–14852
19. Litvinov, R. I., Yakovlev, S., Tsurupa, G., Gorkun, O. V., Medved, L., and Weisel, J. W. (2007) Direct evidence for specific interactions of the fibrinogen αC-domains with the central E region and with each other. *Biochemistry* **46,** 9133–9142
20. Weisel, J. W. (2005) Fibrinogen and Fibrin. *Adv. Protein Chem.* **70,** 247–299
21. Yang Z., Mochalkin, I., and Doolittle, R. F. (2000) A model of fibrin formation based on crystal structures of fibrinogen and fibrin fragments complexed with synthetic peptides. *Proc. Natl. Acad. Sci. U.S.A.* **97,** 14156–14161
22. Holm, B., Nilsen, D. W., Kierulf, P., and Godal, H. C. (1985) Purification and characterization of 3 fibrinogens with different molecular weights obtained from normal plasma. *Thromb. Res.* **37,** 165–176
23. Gorkun, O. V., Henschen-Edman, A. H., Ping, L. F., and Lord, S. T. (1998) Analysis of Aa251 fibrinogen. The αC domain has a role in polymerization, albeit more subtle than anticipated from the analogous proteolytic fragment X. *Biochemistry* **37,** 15434–15441
24. Yermolenko, I. S., Lishko, V. K., Ugarova, T. P., and Magonov, S. N. (2011) High-resolution visualization of fibrinogen molecules and fibrin fibers with atomic force microscopy. *Biomacromolecules* **12,** 370–379
25. Ugarova, T. P., Budzynski, A. Z., Shattil, S. J., Ruggeri, Z. M., Ginsberg, M. H., and Plow, E. F. (1993) Conformational changes in fibrinogen elicited by its interaction with platelet membrane glycoprotein GPIIb-IIIa. *J. Biol. Chem.* **268,** 21080–21087
26. de Maat, M. P., and Verschuur, M. (2005) Fibrinogen heterogeneity. Inherited and noninhereted. *Curr. Opin. Hematol.* **12,** 377–383
27. Lipinska, I., Lipinski, B., Gurewich, V., and Hoffmann, K. D. (1976) Fibrinogen heterogeneity in cancer, in occlusive vascular disease, and after surgical procedures. *Am. J. Clin. Pathol.* **66,** 958–966
28. Gurewich, V., and Lipinska, I. (1981) Lower molecular weight fibrinogen and non-clottable fibrinogen derivatives in diabetes mellitus. *Thromb. Res.* **22,** 535–541
29. Lipinski, B., Lipinska, I., and Nowak, A. (1977) Abnormal fibrinogen heterogeneity and fibrinolytic activity in advanced liver disease. *J. Lab. Clin. Med.* **90,** 187–194
30. Tsurupa, G., Tsonev, L., and Medved, L. (2002) Structural organization of the fibrin(ogen) αC domains. *Biochemistry* **41,** 6449–6459
31. Burton, R. A., Tsurupa, G., Medved, L., and Tjandra, N. (2006) Identification of an ordered compact structure within the recombinant bovine fibrinogen αC-domain by NMR. *Biochemistry* **45,** 2257–2266
32. Weisel, J. W., and Medved, L. (2001) The structure and function of the αC domains of fibrinogen. *Ann. N.Y. Acad. Sci.* **936,** 312–327
33. Tsurupa, G., Hantgan, R. R., Burton, R. A., Pechik, I., Tjandra, N., and Medved, L. (2009) Structure, stability, and interaction of the fibrin(ogen) αC-domains. *Biochemistry* **48,** 12191–12201
34. Rudee, M. L., and Price, T. M. (1981) Observation of the α-chain extensions of fibrinogen through a new electron miscroscope specimen preparation technique. *Ultramicroscopy* **7,** 193–195
35. Schielen, W. J., Voskuilen, M., Tesser, G. I., and Nieuwenhuizen, W. (1989) The sequence A-α-(148–160) in fibrin, but not in fibrinogen is accessible to monoclonal antibodies. *Proc. Natl. Acad. Sci. U.S.A.* **86,** 8951–8954
36. Yakovlev, S., Makogonenko, E., Kurochkina, N., Nieuwenhuizen, W., Ingham, K., and Medved, L. (2000) Conversion of fibrinogen to fibrin. Mechanism of exposure of t-PA and plasminogen binding sites. *Biochemistry* **39,** 15730–15741
37. Tsurupa, G., Yakovlev, S., McKee, P., and Medved, L. (2010) Noncovalent interaction of α2-antiplasmin with fibrin(ogen). Localization of α2-antiplasmin-binding sites. *Biochemistry* **49,** 7643–7651
38. Zamarron, C., Ginsberg, M. H., and Plow, E. F. (1990) Monoclonal anti-

bodies specific for a conformationally altered state of fibrinogen. *Thromb. Haemost.* **64,** 41–46
39. Lishko, V. K., Kudryk, B., Yakubenko, V. P., Yee, V. C., and Ugarova, T. P. (2002) Regulated unmasking of the cryptic binding site for integrin $\alpha_M\beta_2$ in the γC-domain of fibrinogen. *Biochemistry* **41,** 12942–12951
40. Evans-Nguyen, K. M., Fuierer, R. R., Fitchett, B. D., Tolles, L. R., Conboy, J. C., and Schoenfisch, M. H. (2006) Changes in adsorbed fibrinogen upon conversion to fibrin. *Langmuir* **22,** 5115–5121
41. Wigren, R., Elwing, H., Erlandsson, R., Welin, S., and Lundström, I. (1991) Structure of adsorbed fibrinogen obtained by scanning force microscopy. *FEBS Lett.* **280,** 225–228
42. Koo, J., Rafailovich, M. H., Medved, L., Tsurupa, G., Kudryk, B. J., Liu, Y., and Galanakis, D. K. (2010) Evaluation of fibrinogen self-assembly. Role of its αC region. *J. Thromb. Haemost.* **8,** 2727–2735
43. Lishko, V. K., Yermolenko, I. S., and Ugarova, T. P. (2010) Plasminogen on the surface of fibrin clot prevents adhesion of leukocytes and platelets. *J. Thromb. Haemost.* **8,** 799–807
44. Mills, D., and Karpatkin, S. (1971) The non-plasmin, proteolytic origin of human fibrinogen heterogeneity. *Biochim. Biophys. Acta* **251,** 121–125
45. Holm, B., and Godal, H. C. (1984) Quantitation of the three normally occurring plasma fibrinogens in health and during so-called "acute phase" by SDS electrophoresis of fibrin obtained from EDTA-plasma. *Thromb. Res.* **35,** 279–290
46. Owen, J., Friedman, K. D., Grossman, B. A., Wilkins, C., Berke, A. D., and Powers, E. R. (1987) Quantitation of fragment X formation during thrombolytic therapy with streptokinase and tissue plasminogen activator. *J. Clin. Invest.* **79,** 1642–1647
47. Hanss M., Biot F. (2001) A database for human fibrinogen variants. *Ann. N.Y. Acad. Sci.* **936,** 89–90
48. Hayes, T. (2002) Dysfibrinogenemia and thrombosis. *Arch. Pathol. Lab. Med.* **126,** 1387–1390
49. Kollman, J. M., Pandi, L., Sawaya, M. R., Riley, M., and Doolittle, R. F. (2009) Crystal structure of human fibrinogen. *Biochemistry* **48,** 3877–3886